Cell Metabolism
Article

The REGγ Proteasome Regulates Hepatic Lipid Metabolism through Inhibition of Autophagy

Shuxian Dong,[1,3,8] Caifeng Jia,[1,8] Shengping Zhang,[1,8] Guangjian Fan,[1] Yubing Li,[1] Peipei Shan,[1] Lianhui Sun,[1] Wenzhen Xiao,[1] Lei Li,[1] Yi Zheng,[1] Jinqin Liu,[1] Haibing Wei,[1] Chen Hu,[1] Wen Zhang,[2] Y. Eugene Chin,[4] Qiwei Zhai,[5] Qiao Li,[6] Jian Liu,[3] Fuli Jia,[3] Qianxing Mo,[3] Dean P. Edwards,[3] Shixia Huang,[3] Lawrence Chan,[3] Bert W. O'Malley,[3] Xiaotao Li,[1,3,*] and Chuangui Wang[1,7,*]

[1]Shanghai Key Laboratory of Regulatory Biology, Institute of Biomedical Sciences
[2]Department of Chemistry
East China Normal University, Shanghai, 200241, China
[3]Department of Molecular and Cellular Biology, Department of Medicine, The Dan L. Duncan Cancer Center, The Diabetes Research Center, Baylor College of Medicine, One Baylor Plaza, Houston, TX 77030, USA
[4]Institute of Health Sciences, Shanghai Institutes of Biological Sciences, Chinese Academy of Sciences, Shanghai, 200025, China
[5]Key Laboratory of Nutrition and Metabolism, Institute for Nutritional Sciences, Shanghai Institutes for Biological Sciences, Chinese Academy of Sciences, Shanghai, 200031, China
[6]Departments of Pathology and Laboratory Medicine, University of Ottawa, Ottawa, ON K1H 8M5, Canada
[7]Guangxi Collaborative Innovation Center for Biomedicine and Drug Discovery, Guangxi Medical University, Nanning, Guangxi 530021, China
[8]These authors contributed equally to this work
*Correspondence: xiaotaol@bcm.edu (X.L.), cgwang@bio.ecnu.edu.cn (C.W.)
http://dx.doi.org/10.1016/j.cmet.2013.08.012

SUMMARY

The ubiquitin-proteasome and autophagy-lysosome systems are major proteolytic pathways, whereas function of the Ub-independent proteasome pathway is yet to be clarified. Here, we investigated roles of the Ub-independent REGγ-proteasome proteolytic system in regulating metabolism. We demonstrate that mice deficient for the proteasome activator REGγ exhibit dramatic autophagy induction and are protected against high-fat diet (HFD)-induced liver steatosis through autophagy. Molecularly, prevention of steatosis in the absence of REGγ entails elevated SirT1, a deacetylase regulating autophagy and metabolism. REGγ physically binds to SirT1, promotes its Ub-independent degradation, and inhibits its activity to deacetylate autophagy-related proteins, thereby inhibiting autophagy under normal conditions. Moreover, REGγ and SirT1 dissociate from each other through a phosphorylation-dependent mechanism under energy-deprived conditions, unleashing SirT1 to stimulate autophagy. These observations provide a function of the REGγ proteasome in autophagy and hepatosteatosis, underscoring mechanistically a crosstalk between the proteasome and autophagy degradation system in the regulation of lipid homeostasis.

INTRODUCTION

Macroautophagy (hereafter referred to as autophagy) is a conserved degradative process that is essential for cellular homeostasis and quality control and mediates degradation of damaged or excess proteins and organelles in lysosomes (Mizushima, 2007). Its dysregulation is involved in many physiological disorders and human diseases (Mizushima, 2007). Recent studies reveal that autophagy is required for breakdown of lipid droplets, and inhibition of autophagy leads to steatosis and fatty liver in mice (Czaja, 2010; Singh et al., 2009). Autophagy also regulates adipocyte differentiation and fat storage (Zhang et al., 2009). These findings present autophagy as a therapeutic target that could potentially be manipulated to treat diseases accompanied by excess lipid accumulation (Singh and Cuervo, 2012). Nevertheless, regulatory factors linking autophagy and lipid metabolisms urgently await discovery.

SirT1 (yeast Sir2) is a protein deacetylase that acts as a master metabolic sensor of NAD+ and has been reported to modulate lifespan and cellular metabolism (Guarente, 2000). SirT1 reduces fat accumulation in white adipose (Picard et al., 2004) and promotes browning of white adipose (Qiang et al., 2012). SirT1 overexpression reduces high-fat diet (HFD)-induced steatosis and improves insulin sensitivity (Pfluger et al., 2008), whereas loss of SirT1 leads to liver steatosis and inflammation (Purushotham et al., 2009). In addition, SirT1 provides a cell survival advantage in response to stress by deacetylating a number of substrates, such as p53 (Luo et al., 2001) and FOXOs (Brunet et al., 2004). SirT1 can be regulated by FOXO3a, p53, and HIC1 at the level of transcription (Chen et al., 2005; Nemoto et al., 2004) and is regulated by DBC1 through protein-protein interaction (Zhao et al., 2008). SirT1 expression is augmented following fasting (Nemoto et al., 2004). We previously reported that DNA damaging agents also induce SirT1 expression (Wang et al., 2006). Importantly, overexpression of SirT1 stimulates autophagy, and SirT1 knockout (KO) MEF cells cannot fully activate autophagy under starved conditions (Lee et al., 2008). However, molecular factors and mechanisms that control SirT1 autophagic function are largely unexplored.

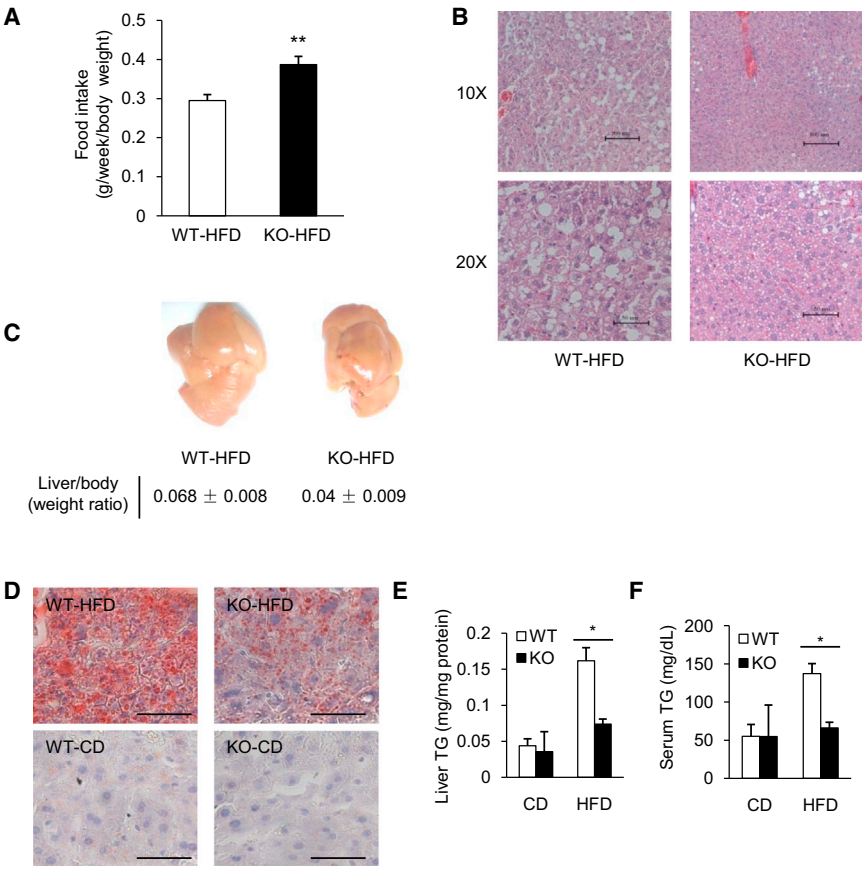

Figure 1. REGγ Regulates Fat Accumulation, and REGγ-Deficient Mice Are Protected from High-Fat Diet-Induced Liver Steatosis

(A) Food intake of wild-type (WT) or REGγ-knockout (KO) male mice on HFD (n = 4). REGγ-KO mice exhibited increased food consumption. Data represent mean ± SD, **p < 0.01.

(B and C) REGγ-KO mice are protected against HFD-induced liver steatosis. Livers were examined in mice fed with HFD for 19 weeks. (B) Liver tissues were stained with hematoxylin and eosin (H&E). Pictures were taken using a microscopy with 10× and 20× object lenses. The lipid droplets appeared as uncolored circles in the HE stained tissue slide. (C) Representative liver images (upper panel) and liver/body weight ratios (lower panel) after 19 weeks of HFD feeding.

(D) Representative images for oil red O staining of lipid droplet accumulation in frozen liver sections of mice fed with standard chow diet (CD) or HFD for 19 weeks (scale bar, 50 μm).

(E and F) Total triglyceride (TG) levels in liver (E) and serum (F) of mice fed with CD or HFD for 19 weeks. Data represent mean ± SD (n = 3), *p < 0.05. See also Figure S1.

The proteasome is a large protein complex consisting of a 20S proteolytic core and three proteasomal activators, 19S (or PA700), 11S (or PA28, REG), and PA200. The 19S activator binds to the 20S core and primarily mediates degradation of ubiquitinated proteins. The 11S activator binds to the proteasome and mainly promotes Ub-independent degradation. However, little attention has been paid to the Ub-independent proteolysis in eukaryotes. Our investigations have revealed that REGγ (or PA28γ), one of the 11S proteasomal activators (Dubiel et al., 1992; Ma et al., 1992), promotes Ub-independent degradation of SRC-3 and p21 (Li et al., 2006, 2007). In this study, we found that REGγ knockout (REGγ-KO) mice exhibit autophagy and are protected against HFD-induced liver steatosis through enhanced autophagy. REGγ also serves as a master regulator in switch off/on autophagy under normal and energy-deprivation conditions by regulating SirT1. Our findings suggest that REGγ is a potential therapeutic target for disordered lipid metabolism.

RESULTS

REGγ Plays a Role in Regulating Lipid Metabolism and HFD-Induced Liver Steatosis

REGγ-KO mice were reported to display reduced body weight and growth retardation (Barton et al., 2004; Murata et al., 1999). This prompted us to investigate the functional role of REGγ in metabolism. To determine if and how REGγ expression impacts lipid metabolism in vivo, we challenged REGγ-KO mice with a HFD. Interestingly, we observed a slightly increased food intake in REGγ-KO mice on HFD (Figure 1A). Loss of REGγ had a significant beneficial effect in mice, preventing them from developing liver steatosis after 19 weeks of HFD (Figures 1B and 1C) in comparison with the wild-type (WT) littermates, despite the fact that they had similar weight gains during HFD feeding (Figure S1A). Differential lipid metabolism in these mice was further demonstrated by classic oil red O staining of livers, showing that the REGγ-KO mice exhibited a marked reduction of HFD-induced hepatic lipid accumulation (Figure 1D, upper panel); mice with standard chow diet (CD) had few noticeable changes (Figure 1D, lower panel). Quantification of the liver and serum triglyceride (TG) levels in mice confirmed that REGγ-KO mice were resistant to HFD-induced liver steatosis (Figures 1E and 1F). These data support that REGγ-KO mice are protected from HFD-induced hepatic steatosis.

In addition, REGγ overexpression led to an increase of total lipid accumulation as well as an increase in size of lipid droplets in human hepatocellular carcinoma (HepG2) cells, effects that are further exaggerated after oleate treatment (Figure S1B), whereas transient overexpression of REGα or REGβ, two homologous proteasome activators (Dubiel et al., 1992; Ma et al., 1992), had no such effect (Figure S1C). Collectively, the above data revealed a role for REGγ in regulating hepatic lipid metabolism and a protective outcome against HFD-induced liver steatosis in REGγ-KO mice.

Deficiency of REGγ Triggers Autophagy

To clarify the effect of REGγ on lipid metabolism, we examined mRNA expression of a number of lipid transport, lipogenesis, and fatty acid oxidation genes in the liver of REGγ-WT and -KO mice (Figure S1D). However, there was no significant

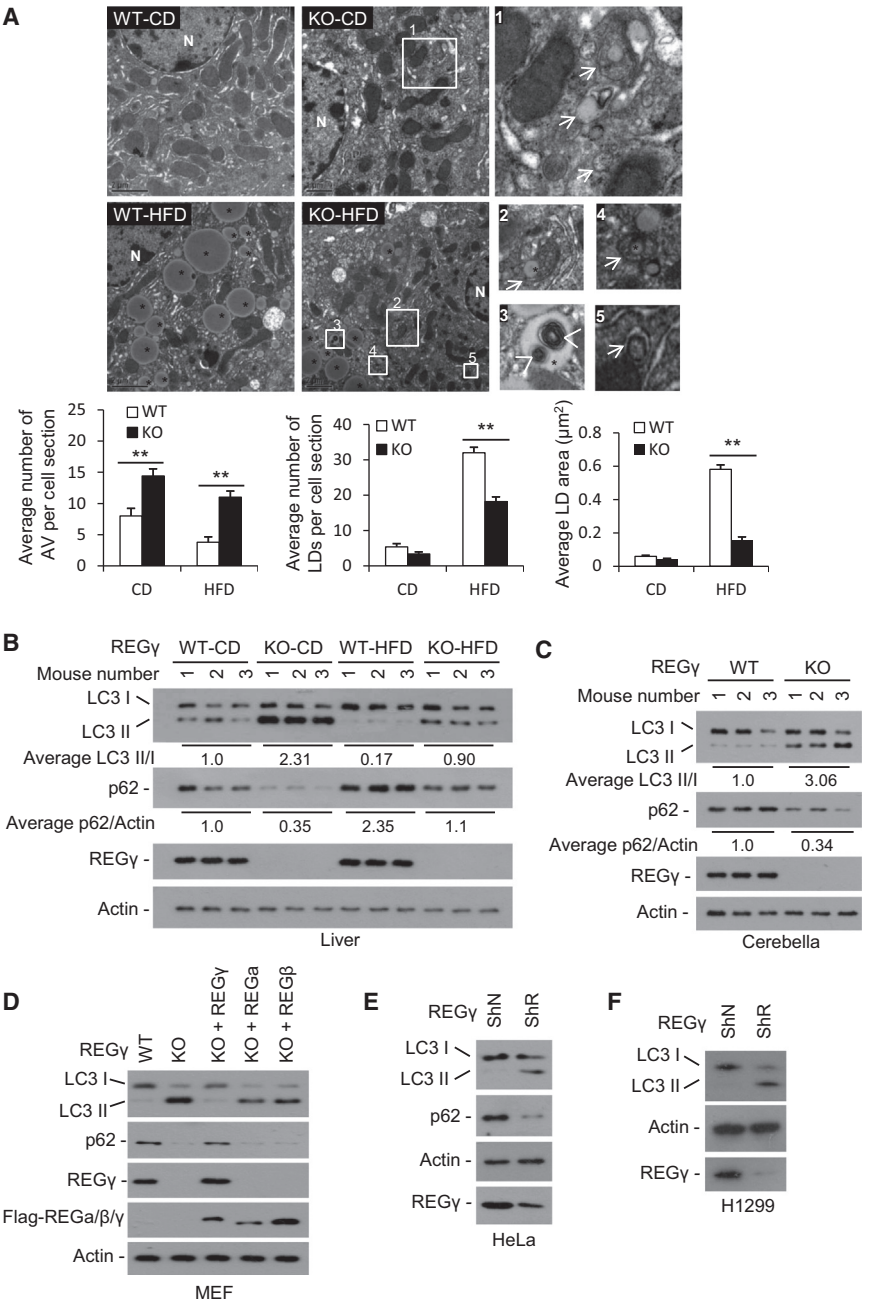

Figure 2. REGγ Deficiency Triggers Autophagy

(A) Transmission electron microscopy of liver tissues from REGγ-WT and -KO mice (n = 3) with CD or HFD for 19 weeks. * indicates lipid droplet (LD) (bright round organelle). Images 1–5 are high magnifications of the "white box" areas indicated in the images of KO-CD and KO-HFD. The arrows show autophagic vacuoles (AVs) containing LDs, other cargos, or mixed cargos; the arrow heads show AVs in LDs. The average numbers and sizes of AVs and LDs were quantified (lower panels). The average number of AVs, lipid numbers, and lipid size were determined from a randomly selected pool of 5–10 fields under each condition. Data represent mean ± SD, $^{**}p < 0.01$.

(B and C) The protein levels of autophagy markers p62 and LC3 in livers (B) and cerebellums (C) of three pairs of REGγ-WT and -KO mice maintained on a standard CD or HFD for 19 weeks were determined by western blot. The relative average levels of LC3-II/I or p62/actin under each condition were quantified by densitometry of immunoblot signals and are presented below the blots.

(D) The protein levels of LC3 and p62 in REGγ-WT and -KO MEF cell lines were detected by western blot. To determine the specific effect for REGγ, REGγ-KO MEF cells were infected with lentiviral vectors expressing Flag-tagged REGγ, REGα, or REGβ for 48 hr.

(E and F) Protein levels of LC3 and p62 in HeLa and H1299 cells with stable knockdown of REGγ (ShR) or a vector control (ShN) were determined by western blot. See also Figure S2.

change in the expression of selected genes between REGγ-WT and -KO mouse livers. Next, we examined fatty acid uptake, lipid synthesis, and fatty acid β-oxidation in primary hepatic cells from livers of REGγ-WT and -KO mice. The REGγ-deficient hepatic cells showed no significant alterations in fatty acid uptake or lipid synthesis, but exhibited a slight but significant increase in fatty acid β-oxidation after pretreatment with fatty acids (Figures S1E–S1G). These data suggest that the protection of HFD-induced hepatic steatosis in REGγ-KO mice is likely associated with increased lipid oxidation.

Recent studies reveal that autophagy promotes lipid droplet breakdown and the rate of fatty acid β-oxidation increased during lipid loading, but to a much lesser extent in cells with inhibited autophagy (Singh et al., 2009). Moreover, autophagy is critical for β-oxidation of fatty acids in the liver (Sinha et al., 2012). Therefore, we tested whether REGγ regulates liver steatosis via autophagy. Transmission electron microscopic analysis of liver autophagy in REGγ-WT and -KO mice revealed that REGγ knockout led to a marked increase of the number of autophagic vacuoles (AVs) in vivo (Figure 2A). Mice fed a HFD have reduced hepatic autophagy (Yang et al., 2010). Similarly, our data showed the number of AVs in liver sections decreased after HFD treatment, but the number of AVs in HFD-treated REGγ-KO mice still maintain at a certain level in comparison with REGγ-WT mice on HFD. In addition, we also observed AVs that enwrapped lipid droplets (Figure 2A #2 and #4) or mixed lipid droplets and AVs (Figure 2A #3) in liver sections of REGγ-KO mice on HFD. HFD-treated REGγ-WT mice displayed robust accumulation of large lipid droplets, whereas HFD-fed REGγ-KO mice showed a marked reduction of both the number and the size of lipid droplets (Figure 2A). These results indicate that REGγ deficiency induces autophagy in mouse liver and that the protection of HFD-induced hepatic steatosis in REGγ-KO mice may result from increased autophagy.

Next, we examined the levels of autophagy markers in the livers of REGγ-KO and -WT mice fed with CD or HFD for 19 weeks (Figure 2B). Results showed a remarkably increased LC3-II and a clearly decreased p62 in REGγ-KO livers with a standard CD. HFD led to a marked decrease in LC3-II and an accumulation of p62 in both REGγ-WT and -KO mouse livers, but HFD-treated REGγ-KO mice still maintain higher autophagy levels than REGγ-WT mice with HFD, indicating that autophagy levels are always higher in REGγ-KO mice than in WT at given diet. In addition, REGγ-KO mice exhibited a decreased p62 and an increased LC3-II in cerebellum (Figure 2C). Reduced p62 and enhanced LC3-II were also observed in REGγ-KO MEF cells as well as HeLa and H1299 cells with REGγ stable knockdown (Figures 2D–2F). Moreover, expression of an RNAi-resistant REGγ, but not REGα/β, restored REGγ deficiency-induced autophagy, indicating the specificity of REGγ in its inhibition of autophagy (Figure 2D).

To further assess the role of REGγ in autophagy, we evaluated autophagic flux in REGγ-WT and -KO MEFs treated with or without bafilomycin A1 (Ba), which inhibits fusion between autophagosomes and lysosomes (Figure S2A). Results showed that in the presence of Ba, loss of REGγ also results in an increased accumulation of LC3-II under both normal and starvation conditions, indicating that the differences in LC3-II levels in REGγ-WT and -KO MEF cell lines were due to autophagic induction rather than a blockade at downstream steps. The inhibitory effect of REGγ on autophagy was further confirmed by quantitation of GFP-LC3 puncta formation. REGγ-deficient cells displayed an increase in both the number of punctate LC3 per cell and the GFP-LC3 punctae-positive cells (Figures S2B and S2C). Therefore, normal REGγ expression keeps autophagy at a low level under basal conditions.

REGγ Inhibits Autophagy in a SirT1-Dependent Manner under Normal Conditions

Previous studies demonstrate that suppression of the ubiquitin proteasome system induces ER stress, and autophagy can be activated by ER stress (Ding et al., 2007a). Moreover, ER stress contributes to metabolic dysfunction and hepatic steatosis, and a fundamental change is observed in hepatic ER function in obesity from protein to lipid synthesis and metabolism (Fu et al., 2011, 2012). To assess whether ER stress may be involved in REGγ deficiency-induced autophagy and hepatic steatosis resistance, we examined the status of ER homeostasis in REGγ-KO or -knockdown cells in the presence or absence of an ER stress inducer, thapsigargin (Figures S2D–S2F). Nevertheless, REGγ deficiency exhibited no significant effect due to ER stress under normal or thapsigargin-treated conditions. These results suggest that REGγ deficiency-induced autophagy is not likely due to ER stress.

To understand the molecular basis of REGγ-mediated regulation of autophagy, we carried out a large-scale proteomic screen using antibody array (Fullmoon Biosystems Inc.) and a reverse-phase protein array (RPPA) to identify proteins differentially regulated in REGγ-positive and REGγ null MEF cells (X.L. and S.H., unpublished work). The Fullmoon arrays contain antibodies against phospho and total proteins (Bernier et al., 2011), and RPPA assays include additional proteins not present in the Fullmoon array, together covering nearly 1,400 proteins in more than 30 different pathways. In the RPPA analysis, we discovered that SirT1 enhancement in REGγ null MEFs was statistically significant, similar to the significant changes in the positive controls of the known REGγ targets, p53 and p21, in REGγ null MEFs (Figure S3A). The fact that REGγ-KO triggers autophagy (Figure 2) and SirT1 overexpression stimulates autophagy motivated us to test whether REGγ affects autophagy by negatively regulating SirT1.

First, we assessed whether REGγ interacts with SirT1. Results showed that SirT1 coprecipitated with REGγ in 293T cells overexpressing GFP-REGγ and Flag-SirT1 (Figure 3A). Endogenous REGγ binds to SirT1 but not other sirtuins such as SirT2 (Figure 3B). The direct association between REGγ and SirT1 was verified in vitro (Figure 3C). Moreover, a region of SirT1 (aa 378–458) within the catalytic domain and a region corresponding to aa 66–103 in REGγ is essential for REGγ-SirT1 interaction (Figures S3B and S3C). These results indicate that REGγ is a SirT1-interacting protein.

Next, we evaluated whether REGγ regulates autophagy via SirT1. Concomitant expression of REGγ inhibited SirT1-induced conversion of LC3-I to LC3-II (Figure 3D) and formation of GFP-LC3 punctae (Figures 3E and 3F). Increased LC3-II and reduced p62 were observed in REGγ-only knockdown cells, but not in cells with REGγ/SirT1 double knockdown (Figure 3G). In parallel, REGγ knockdown increased the number of LC3 punctae per cell and GFP-LC3 punctae-positive cells, whereas REGγ/SirT1 double knockdown exhibited little change in the number of the LC3 punctae and the percentage of punctae-positive cells (Figures 3H and 3I). These results indicate that endogenous SirT1 is required for REGγ deficiency-induced autophagy.

REGγ Mediates Ub-Independent Degradation of SirT1

Next, we examined whether REGγ is involved in SirT1 degradation. Results showed a strong negative correlation between REGγ and SirT1 expression in vivo (Figures 4A and 4B). Stable knockdown of REGγ results in elevated SirT1 expression (Figure 4C). We also observed increased SirT1 expression in REGγ-KO MEF cells, and restoration of REGγ expression in these cells repressed SirT1 expression (Figure 4D). However, REGγ deficiency had no effect on *SirT1* transcript levels (Figure 4E). Moreover, REGγ overexpression instigated a reduction of endogenous SirT1 protein (Figure 4F) and increased SirT1 degradation (Figure 4G). In contrast, the rate of SirT1 decay was markedly delayed in both REGγ-knockdown HeLa cells (Figure 4H) and REGγ-KO MEFs (Figure 4I), indicating that endogenous REGγ expression renders SirT1 unstable. Using a ts85 cell line, which harbors a thermolabile ubiquitin-activating enzyme that abolishes the transfer of ubiquitin to target proteins at nonpermissive temperatures (37°C) (Li et al., 2007), we observed a slower degradation rate in SirT1 at 37°C compared to that at 30°C, while REGγ overexpression could still promote SirT1 degradation at 37°C (Figure S4A). REGγ overexpression had no effect on SirT1 ubiquitination, whereas treatment with proteasome inhibitor MG132 only mildly increased the level of ubiquitinated SirT1 (Figure S4B). These data indicate that REGγ induces SirT1 degradation in an Ub-independent manner.

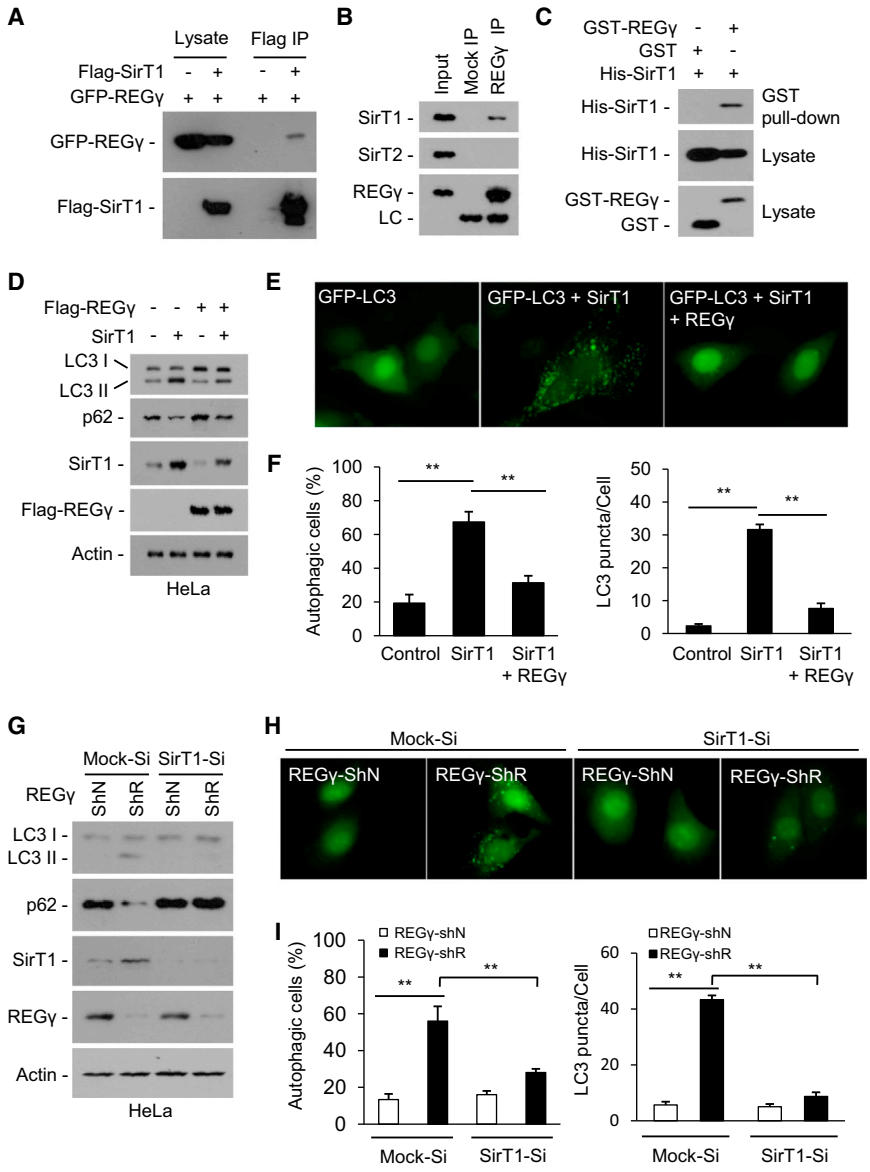

Figure 3. REGγ Inhibits Autophagy in a SirT1-Dependent Manner under Normal Conditions

(A–C) REGγ interacts with SirT1. (A) Flag-SirT1 and GFP-REGγ were expressed in the 293T cells and immunoprecipitated with FLAG-M2 agarose beads, and coprecipitated REGγ was detected by western blot. (B) Endogenous REGγ in HeLa cells was precipitated using anti-REGγ antibody or with IgG (Mock IP), and coprecipitated SirT1 and SirT2 were detected by western blot. (C) REGγ interacts with SirT1 in vitro. His-tagged SirT1 was incubated with GST-REGγ or GST proteins for 4 hr at 4°C. REGγ-SirT1 coprecipitation was determined by GST pull-down and western blot.

(D–F) REGγ inhibits SirT1 autophagic function. (D) HeLa cells were transfected with indicated plasmids for 30 hr. The conversion of LC3-I to LC3-II and levels of p62 were determined by western blot. (E) REGγ inhibits SirT1-stimulated GFP-LC3 punctae formation. HeLa cells seeded on coverslips were transfected with GFP-LC3 and indicated plasmids for 30 hr and GFP-LC3 were visualized by fluorescence microscopy. (F) The percentages of GFP-LC3-positive cells with GFP-LC3 punctae and the GFP-LC3 punctae per cell in (E) were quantified. Data represent mean ± SD, $^{**}p < 0.01$.

(G–I) SirT1 is required for REGγ-deficient induced autophagy. (G) SirT1-knockdown attenuates REGγ-knockdown-induced LC3-II accumulation and p62 reduction. HeLa cells with stable knockdown of SirT1 (SirT1-Si) or control vectors (Mock-Si) were infected with pLL3.7 vector (ShN) or REGγ-knockdown (ShR) lentivirus for 72 hr. Cell lysates were western blotted for SirT1, REGγ, LC3, and p62. (H) SirT1-knockdown represses REGγ-knockdown-induced formation of GFP-LC3 punctae. Cells in (G) were transiently transfected with GFP-LC3 for 20 hr and visualized by fluorescence microscopy. (I) The percentages of GFP-LC3-positive cells with GFP-LC3 punctae and the GFP-LC3 punctae per cell in (H) were quantified. Data represent mean ± SD, $^{**}p < 0.01$. See also Figure S3.

REGγ Inhibits SirT1-Mediated Deacetylation of the Autophagy Machinery

SirT1 stimulates autophagy by deacetylating Atg5, Atg7, and Atg8 (Lee et al., 2008). Since SirT1 is required for REGγ deficiency-induced autophagy (Figures 3G–3I), we hypothesize that REGγ regulates autophagy via SirT1-mediated deacetylation of Atg proteins. As expected, REGγ-KO reduced acetylation levels of Atg5/Atg7 in primary hepatocytes, and pharmacological inhibition of SirT1 with nicotinamide (NAM) blocked REGγ deficiency-induced Atg5/Atg7 deacetylation (Figure 5A). Acetylation of ULK1 (Atg1) (Lin et al., 2012) and Atg3 promote autophagy (Yi et al., 2012). However, Atg5/Atg7 but not Atg1/Atg3 bind to SirT1 (Figure S5A), and REGγ overexpression could not affect Atg1/Atg3 acetylation (data not shown). Taken together, we believe that SirT1-dependent deacetylation of Atg5/Atg7 contributes to REGγ deficiency-induced autophagy.

Next, we examined whether overexpression of REGγ can alter SirT1 deacetylase activity on Atg5/Atg7. To avoid REGγ-induced degradation of SirT1, increasing amounts of SirT1 expression plasmids (++) were cotransfected with REGγ. Results showed that REGγ inhibited SirT1-mediated deacetylation of Atg5/Atg7 (Figures 5B and 5C), indicating that REGγ directly inhibits SirT1 activity in deacetylating Atg5/Atg7. Interestingly, REGγ has no effect on SirT1-induced deacetylation of p53 (Figure S5B), suggesting a specific role for REGγ in regulating of autophagy complex.

To further address why REGγ selectively inhibits SirT1-induced deacetylation of Atg5/Atg7, we checked whether REGγ competes with Atg proteins for SirT1 binding. Overexpression of REGγ inhibited SirT1 binding to Atg5/Atg7 (Figures 5D and 5E). Restoring expression of REGγ in REGγ-KO MEF cells reduced endogenous SirT1-Atg7 interaction under low dose of MG132 treatment (Figure S5C). REGγ also displaces Atg7 from

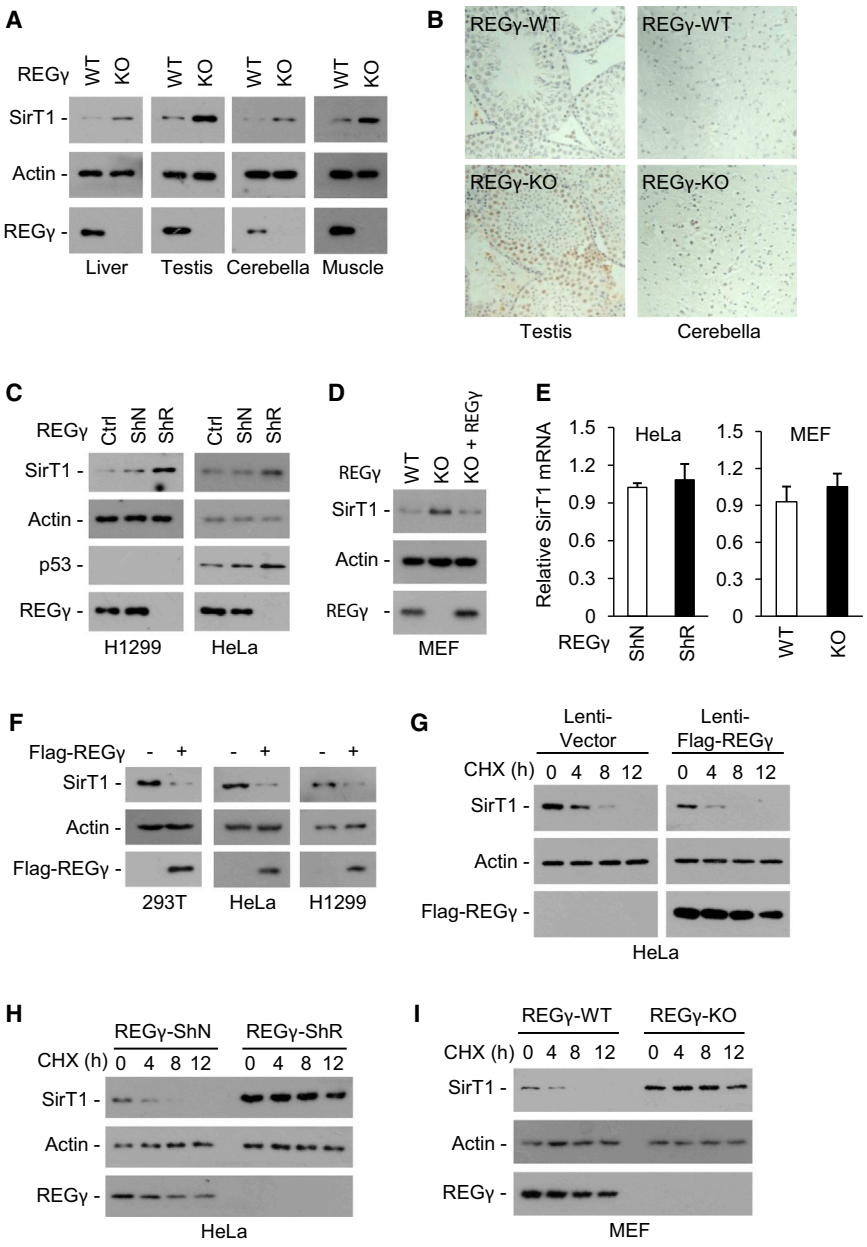

Figure 4. REGγ Mediates Degradation of SirT1

(A–E) REGγ deficiency causes accumulation of endogenous SirT1. (A and B) SirT1 protein levels in liver, testis, cerebellum, and muscle tissues of REGγ-WT and -KO mice were examined by western blot (A) and immunohistochemical staining (B). (C) H1299 and HeLa cells were stably infected with control lentivirus (ShN) or lentivirus expressing REGγ siRNA (ShR) and analyzed for REGγ, SirT1, and p53 expression levels by western blot. (D) MEFs from REGγ-WT and -KO mice were analyzed for REGγ and SirT1 expression levels by western blot. To restore REGγ expression, REGγ-KO MEFs were infected with a lentiviral vector expressing REGγ for 48 hr. (E) Relative mRNA expression of SirT1 in REGγ-deficient cells was examined by quantitative real-time PCR analysis. Data represent mean ± SD (n = 3).

(F) 293T, HeLa, and H1299 cells were transfected with a control vector or Flag-REGγ plasmid for 36 hr; cell extracts were subjected to western blotting.

(G–I) REGγ promotes SirT1 degradation. HeLa cells infected with control lentivirus or lentivirus overexpressing REGγ for 24 hr (G), HeLa cells stably expressing a control lentivirus (ShN) or a lentiviral REGγ shRNA (ShR) (H), or MEFs cells from REGγ-WT and -KO mice (I) were treated with translation inhibitor cycloheximide (CHX, 50 μg/ml) and analyzed for SirT1 stability by western blot. See also Figure S4.

SirT1 in vitro in a dose-dependent manner (Figure 5F). These results suggest that REGγ-induced SirT1-Atg5/Atg7 dissociation also contributes to its inhibitory effect on autophagy.

The above data strongly endorse a specific inhibitory effect of REGγ on SirT1-mediated Atg5/Atg7 deacetylation. Paradoxically, REGγ is mostly localized in nucleus, while Atg5/Atg7 proteins are largely cytosolic. Therefore, we examined how SirT1 mediates functional links between the REGγ and Atg5/Atg7 in mouse primary hepatocytes. Results from immunostaining showed that both REGγ and SirT1 were localized primarily in the nucleus (Figure S5D). Most of the previous studies observed REGγ primarily localized in nucleus, whereas a few studies also showed a cytoplasm-localized REGγ (Wójcik, 1999). We observed that a small fraction of REGγ localized into the cytoplasm, lack of REGγ leads to an accumulation of SirT1 not only in nucleus but also in cytoplasm, and Atg5/Atg7 are found in both the cytoplasm and nucleus (Figure S5D). These results suggest that each of these proteins might dynamically shuttle between nucleus and cytoplasm, although major localization and competition could be in one or two compartments.

Next, we determined in vivo regulation of Atg5/Atg7 acetylation by REGγ (Figure 5G). Results showed that REGγ deficiency markedly reduced hepatic acetylation levels of Atg5/Atg7 in both CD- and HFD-treated mice. HFD treatment increased levels of Atg5/Atg7 acetylation, but HFD-induced hepatic accumulation of acetyl-Atg5/Atg7 is much less in REGγ-KO mice in comparison with WT mice. These results indicate that the REGγ-SirT1-Atg-autophagy signaling pathway is involved in regulating HFD-induced hepatic steatosis in vivo. Taken together, our data suggest that REGγ binds to SirT1, promotes SirT1 degradation, disrupts the interaction of SirT1-Atg5/Atg7, and specifically inhibits SirT1 activity for deacetylating Atg proteins, which then keeps cellular autophagy at a basal level under physiological conditions.

REGγ Controls Hepatic Steatosis through a SirT1- and Autophagy-Dependent Mechanism

Next, we tested whether REGγ regulates hepatic cellular steatosis in a SirT1- and autophagy-dependent manner. We observed

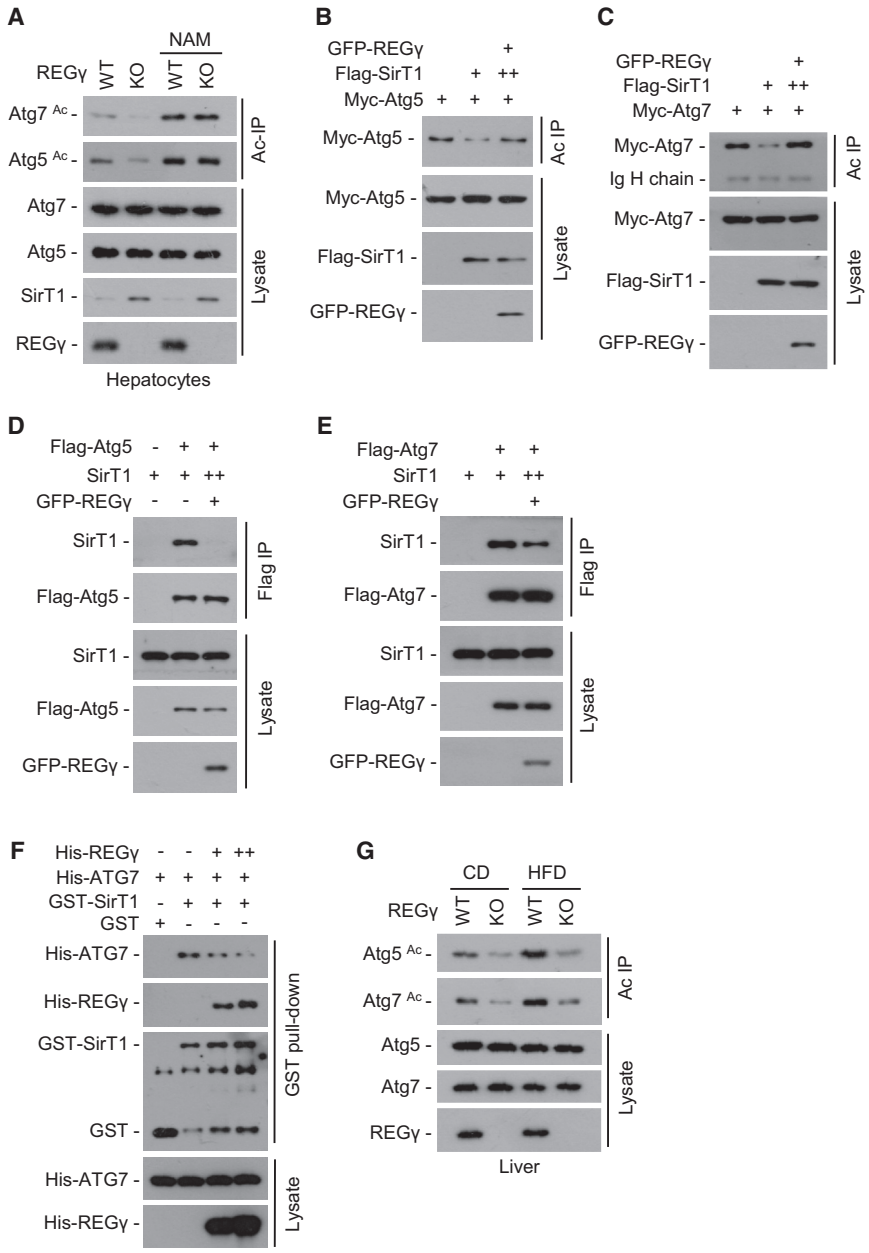

Figure 5. REGγ Regulates SirT1 Autophagic Function by Inhibiting Its Binding to and Deacetylating Autophagy Complex

(A) REGγ regulates acetylation states of Atg5 and Atg7 through SirT1. REGγ-WT and -KO primary hepatocytes were treated with or without NAM (5 mM, 12 hr); cell extracts were immunoprecipitated by anti-acetyl-lysine antibody (Ac IP). The immunoprecipitates were subjected to western blotting with anti-Atg5 or -Atg7 antibody.

(B and C) 293T cells were cotransfected with indicated plasmids and acetylated proteins were immunoprecipitated by anti-acetyl-lysine antibody (Ac IP). To ensure equal expression of SirT1, more SirT1 plasmid DNA (++) was cotransfected with REGγ. The acetylation levels of Atg5/Atg7 protein were determined by western blot using anti-Myc tag antibody.

(D and E) REGγ inhibits SirT1 binding to Atg5/Atg7. 293T cells transfected with indicated plasmids and Flag-tagged Atg5/Atg7 were immunoprecipitated using FLAG-M2 agarose beads followed by western blot. To ensure equal expression of SirT1, more SirT1 plasmid DNA (++) was cotransfected with REGγ.

(F) REGγ inhibits SirT1-Atg7 binding in vitro. GST-SirT1 was incubated with His-Atg7 in the presence or absence of His-REGγ for 4 hr at 4°C, followed by GST pull-down and western blot.

(G) REGγ regulates Atg5 and Atg7 acetylation in vivo. The acetylation status of Atg5 and Atg7 were measured in hepatocytes from REGγ-WT and -KO mice on the CD or HFD for 19 weeks. Liver tissue lysates were immunoprecipitated by anti-acetyl-lysine antibody (Ac IP), and the endogenous acetylation levels of Atg5 and Atg7 proteins were determined by western blot using anti-Atg5 or -Atg7 antibodies. See also Figure S5.

that absence of REGγ was associated with accumulation of LC3-II/SirT1 and reciprocal reduction of p62 in primary hepatocytes isolated from REGγ-KO mice (Figure 6A). REGγ-KO led to a significantly reduced accumulation of intracellular lipids in oleate-palmitate-treated primary hepatocytes, whereas 3-MA (autophagy inhibitor) and NAM (SirT1 inhibitor) both had a significant inhibitory effect on REGγ deficiency-mediated clearance of cellular lipids (Figures 6B and 6C). Similar results were observed in REGγ-knockdown HepG2 cells (Figures S6A–S6C). These data suggest that SirT1 and autophagy are both required for the protective effect against hepatic steatosis in REGγ-deficient mice.

To further address the contributions of autophagy in REGγ deficiency-induced prevention of HFD-induced fatty liver in vivo, REGγ-WT and -KO mice were fed HFD for 7 weeks accompanied with simultaneous intraperitoneal injection of the autophagy inhibitor chloroquine (CLQ) or vehicle during the last 3 weeks. By H&E staining of frozen liver sections and liver TG measurements, we found that 7 weeks of HFD treatment already led to a small but significant increase of lipid droplets and TG levels in livers of REGγ-WT, but not REGγ-KO mice (Figures 6D and 6E). Remarkably, CLQ treatment highly increased accumulation of large lipid droplets and TG levels in livers of both REGγ-KO and -WT mice on HFD. More importantly, the differences between REGγ-WT and -KO mice in levels of TG and lipid droplet accumulation on HFD disappeared following cotreatment with CLQ. The effect of CLQ to inhibit autophagy was confirmed by western blot analysis of LC3-II accumulation (Figure 6F). These results indicate that inhibiting autophagy eliminates the protective roles of REGγ deficiency in HFD-induced liver steatosis, substantiating that autophagy is required for REGγ-mediated regulation of hepatic lipid metabolism. Interestingly, increased REGγ-SirT1 association was observed after oleate treatment (Figure S6D), suggesting that REGγ-SirT1 association may contribute to HFD-induced hepatic steatosis. Collectively, these

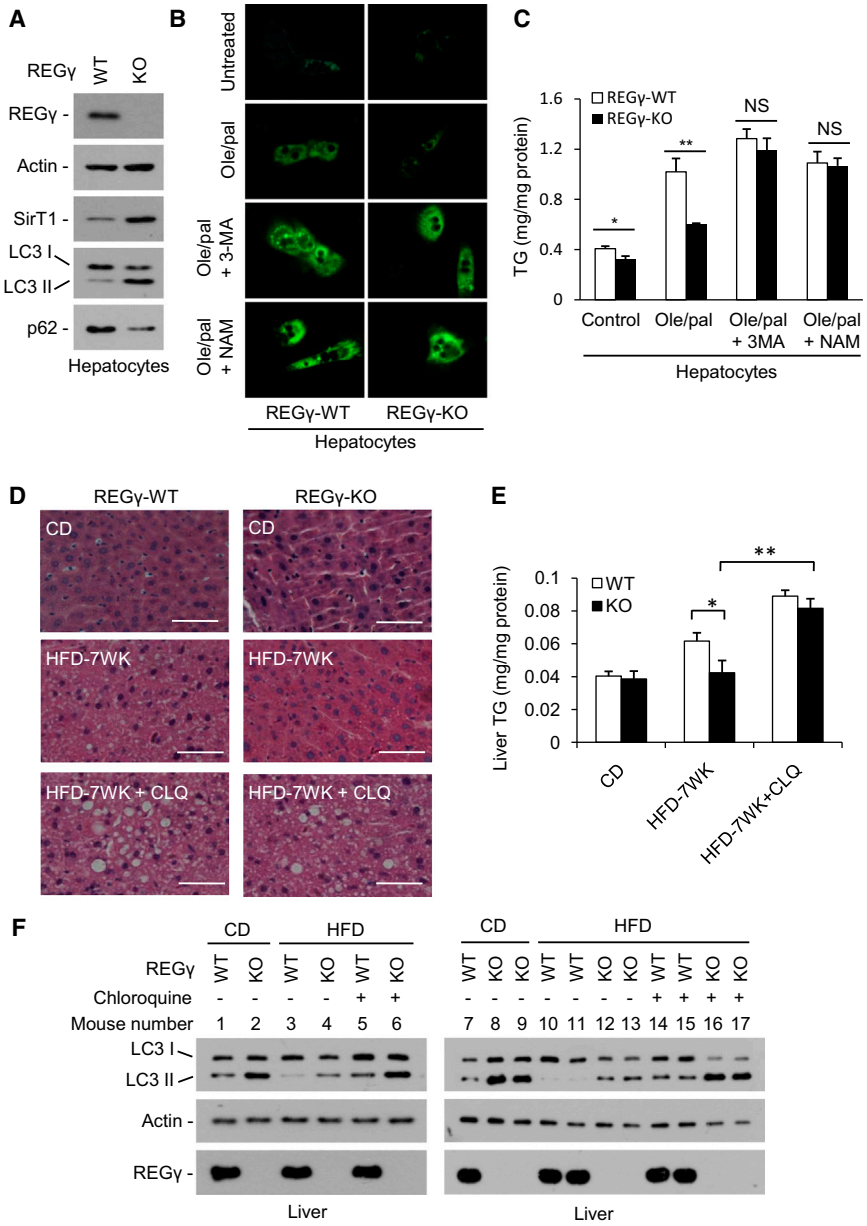

Figure 6. REGγ Deficiency Attenuates Hepatic Steatosis through a SirT1- and Autophagy-Dependent Mechanism

(A) REGγ-KO increased levels of SirT1 and autophagy in hepatocytes. Protein levels of SirT1, p62, and LC3 in primary hepatocytes isolated from REGγ-WT and -KO mice were determined by western blot.

(B) REGγ knockout attenuates fatty acid-induced hepatic cellular steatosis. REGγ-WT and -KO primary hepatocytes were treated with or without 0.3 mM oleate/palmitate (2:1) for 20 hr in the presence of autophagy inhibitor 3-methyladenine (3-MA, 5 mM) or SirT1 inhibitor nicotinamide (NAM, 5 mM), followed by BODIPY 493/503 staining and visualized by fluorescence microscopy.

(C) Cells of (B) were analyzed for total TG levels. Data represent mean ± SD, *$p < 0.05$, **$p < 0.01$, NS = nonsignificant.

(D–F) REGγ-proteasome regulates hepatic lipid metabolism through inhibition of autophagy. REGγ-WT and REGγ-KO mice were fed with standard chow diet (CD) or high-fat diet (HFD) for 7 weeks (mice began on HFD 3 weeks after birth). Four weeks after HFD, mice (n = 3) were treated with intraperitoneal injection of chloroquine (CLQ, 60 mg/kg body weight) every other day along with continued HFD for another 3 weeks. (D) Liver tissues were stained with H&E. Pictures were taken using a microscopy with 20× object lenses. The lipid droplets appeared as uncolored circles in the H&E-stained tissue slide. (E) Total triglyceride (TG) levels of livers in (D) were measured. Data represent mean ± SD (n = 3), *$p < 0.05$, **$p < 0.01$. (F) Liver tissue lysates in (D) were subjected to western blot. CLQ elicits an accumulation of LC3-II in HFD-treated mice, indicating inhibition of autophagy. See also Figure S6.

results demonstrate that the REGγ-proteasome regulates hepatic lipid metabolism through SirT1 and autophagy pathways.

Energy Starvation Dissociates REGγ-SirT1 and Releases SirT1 to Stimulate Autophagy

Autophagy occurs at relatively low levels under basal conditions, but can be induced by a variety of nutrient and intracellular stresses (Kroemer et al., 2010); we therefore examined the impact of starvation on REGγ-SirT1 interactions. As a result, glucose deprivation (GD) significantly reduced REGγ-SirT1 binding (Figure 7A). In parallel, REGγ-SirT1 binding was reduced in cells treated with 2-deoxy-D-glucose (2DG), a potent inhibitor of glucose metabolism that mimics the effect of GD (Figure 7B). In a reciprocal fashion, GD increased the binding of SirT1 to Atg7 (Figure 7C). These results indicate that energy deprivation entails SirT1-REGγ dissociation and thus releases SirT1 to bind to and deacetylate Atg proteins, setting off the autophagic process.

Phosphorylation was found to modulate the function of SirT1 in cell proliferation (Nasrin et al., 2009). To test whether phosphorylation is involved in starvation-induced SirT1-REGγ dissociation, we generated SirT1 phospho-S14-, phospho-T530-, and phospho-T719-specific antibodies (Figure S7A) and examined the effect of GD on SirT1 phosphorylation. Interestingly, GD stimulated SirT1 phosphorylation at T530 and T719, but not S14 (Figure 7D). The AMP-activated protein kinase (AMPK) is activated upon glucose starvation. We found AICAR (AMPK activator) treatment led to a decreased REGγ-SirT1 binding and a concomitant increase in SirT1 phosphorylation at T530 and T719 (Figure 7E). In contrast, treatment of AMPK inhibitor Compound C inhibited GD-induced SirT1 phosphorylation and REGγ-SirT1 dissociation (Figure 7F). These data suggest that AMPK is responsible for glucose starvation-induced SirT1 phosphorylation and REGγ-SirT1 dissociation.

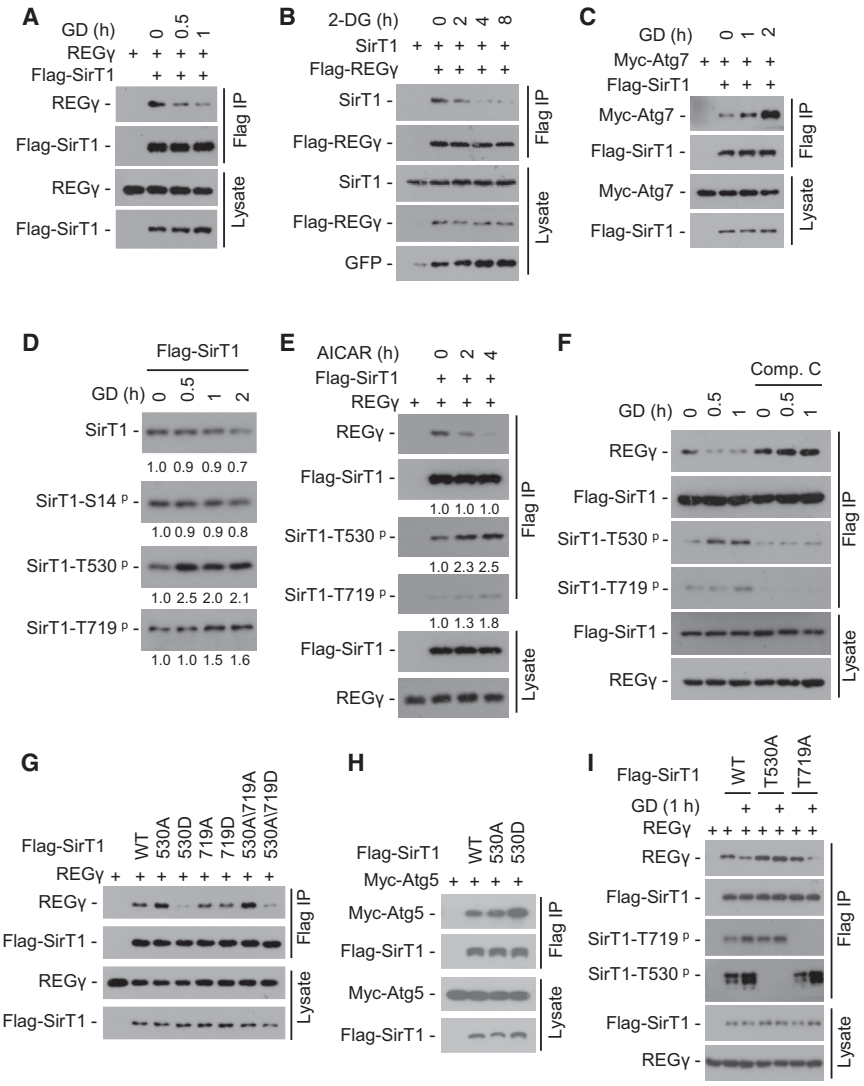

Figure 7. Energy Starvation Dissociates REGγ-SirT1, Unleashing SirT1 to Associate with Atg Proteins for Autophagy Activation

(A) 293T cells were transiently transfected with Flag-SirT1 and REGγ, followed by glucose-free medium (glucose deprivation, GD) treatment. SirT1 was immunoprecipitated using FLAG-M2 beads, and coprecipitation of REGγ was detected by western blot.

(B) 293T cells were transfected with Flag-REGγ, SirT1, and GFP plasmids followed by 2DG (12.5 mM) treatment. REGγ was immunoprecipitated using FLAG-M2 beads, and coprecipitation of SirT1 was detected by western blot.

(C) 293T cells were transiently transfected with Flag-SirT1 and Myc-Atg7, followed by GD treatment. SirT1 was immunoprecipitated using FLAG-M2 beads, and coprecipitated Atg7 was detected by western blot with anti-Myc antibody.

(D) Time course of SirT1 phosphorylation in response to glucose starvation. Flag-SirT1 transfected 293T cells were starved for GD for indicated times. SirT1 was immunoprecipitated with FLAG-M2 beads, and phosphorylation of SirT1 was determined by western blot with antibodies against SirT1 phosphorylation at S14, T530, or T719. Relative levels of phosphorylated and total SirT1 were quantified by densitometry of bands and are presented below the blots.

(E) Activation of AMPK induces SirT1 phosphorylation coupled with REGγ-SirT1 dissociation. Flag-SirT1 and REGγ were transfected into 293T cells for 24 hr, and then cells were treated with or without AMPK activator AICAR (200 μM). SirT1 was immunoprecipitated with FLAG-M2 beads, and the immunoprecipitated complexes were examined by western blot. Relative protein levels were quantified by densitometry of bands and are presented below the blots.

(F) AMPK inhibitor Compound C prevents glucose starvation-induced dissociation of REGγ-SirT1. Flag-SirT1 transfected 293T cells were treated with Compound C (10 μM) for 1 hr, followed by a 0.5–1 hr GD treatment. SirT1 was immunoprecipitated by FLAG-M2 beads, and coprecipitated REGγ were determined by western blot.

(G and H) Phosphorylation-mimetic mutation (T530D) in SirT1 regulates its association with REGγ and Atg5 proteins. Interaction of Flag-SirT1 mutants with REGγ (G) and Atg5 (H) were determined by cotransfection of indicated plasmids into 293T cells, followed by immunoprecipitation using FLAG-M2 beads and western blot.

(I) SirT1 T530 phosphorylation is responsible for GD-induced REGγ-SirT1 dissociation. Flag-SirT1 mutants and REGγ cotransfected 293T cells were treated with or without GD for 1 hr. SirT1 was immunoprecipitated using FLAG-M2 beads, and the immunoprecipitated complexes were examined by western blotting. See also Figure S7.

Sequence analysis reveals that SirT1 T530, but not T719, is highly conserved in human and other species (Figure S7B). We found that SirT1 mutation in T530D, but not in T719D, led to a decreased SirT1-REGγ interaction (Figure 7G), while the SirT1-T530D mutant had an increased association with Atg5 (Figure 7H). Dephosphorylation of SirT1 enhanced its association with REGγ in vitro (Figure S7C). Moreover, the phosphorylation-defective T530A, but not T719A, SirT1 mutant significantly blocked GD-induced REGγ-SirT1 dissociation (Figure 7I). These results demonstrate that glucose starvation stimulates SirT1 phosphorylation mainly at T530 via AMPK, and this modification causes dissociation of SirT1-REGγ coupled with increased association of SirT1-Atg5/Atg7, contributing to liberation of SirT1 to activate autophagy.

DISCUSSION

Results described in this study identify a previously unknown function of the REGγ proteasome in regulating autophagy and lipid metabolism. REGγ deficiency leads to autophagy in vivo and protects mice from HFD-induced liver steatosis. Under normal conditions, REGγ directly binds to SirT1, promotes SirT1 degradation, displaces Atg proteins from SirT1, and increases acetylation of Atg proteins, thereby maintaining autophagy at a lower basal level. Upon energy deprivation, REGγ dissociates from SirT1 in a phosphorylation-dependent manner, unleashing SirT1 to interact with Atg proteins and stimulate autophagy. These observations lead us to propose a role for REGγ as a molecular switch regulating autophagy between normal and

stress conditions (Figure S7D). Furthermore, we revealed that REGγ regulates fatty acid-induced hepatic steatosis through a SirT1- and autophagy-dependent mechanism, and autophagy is essential for REGγ deficiency-mediated prevention of HFD-induced fatty liver.

Cells are equipped with two major proteolytic systems (proteasome and autophagy). Inhibiting autophagy compromises degradation of Ub-proteasome substrates (Korolchuk et al., 2009), whereas proteasome inhibitors activate autophagy, suggesting that the two pathways are functionally coupled (Ding et al., 2007b). The discovery that REGγ deficiency triggers autophagy not only identifies a factor linking proteasomal activity and autophagy, but also defines a function for a proteasome activator in shifting the balance between autophagy and the proteasome system. Since REGγ directs a pathway to degrade certain proteins via an Ub-independent mechanism, our results suggest that cells may use autophagy as an alternative proteolytic pathway when the Ub-independent degradation mechanism is compromised. Recently, we reported that REGγ can be acetylated by CBP, whereas SirT1 can bind with REGγ and deacetylates REGγ, which inhibits heptamerization of REGγ, leading to reduced REGγ capacity (Liu et al., 2013). These observations suggest a mutual regulation between REGγ and SirT1. Previous studies revealed that starvation could induce a slight but significant increase of proteasome activity with no upregulation of ubiquitin-proteasome system (Salem et al., 2007). Given that starvation markedly reduced REGγ-SirT1 interaction, we suggest that the dissociation of SirT1 from REGγ may contribute to starvation-induced increase of proteasome activity through a posttranslational modification regulatory effect. Identification of REGγ-SirT1 complex has established strong bases for continued study of the interplays between proteasome and autophagy under various conditions.

This study also provides insights into the function of the REGγ proteasome in the regulation of lipid homeostasis. We have presented compelling evidence demonstrating the role of REGγ in regulating autophagy via SirT1 under different metabolic conditions and pinpointed the contribution of REGγ in hepatic steatosis and the pathogenesis of fatty liver during HFD feeding. Since inhibiting autophagy by CLQ markedly eliminates the protective roles of REGγ deficiency in HFD-induced liver steatosis in vivo, and SirT1 is required for autophagy stimulation in REGγ-deficient cells, we believe that lipid metabolism can be regulated through the REGγ-SirT1-autophagy pathway. However, our study does not exclude other additional mechanisms mediating REGγ function in lipid homeostasis. Interestingly, we found that fatty acid stimulates REGγ-SirT1 association. Further study on the correlations between SirT1 and REGγ under different metabolic conditions may provide guidance for the treatment of certain types of metabolic disease.

The REG (or PA28) proteasome activators comprise three members: α, β, and γ. REGα/β primarily localize in cytoplasm and regulate immunopeptide generation, whereas REGγ primarily localizes in nucleus and mainly regulates Ub-independent degradation of subsets of proteins. A recent study demonstrated that removal of all three PA28/REG subunits (Triple-REG-KO) decreased hepatic insulin signaling and resulted in minor hepatic steatosis under normal diet condition (Otoda et al., 2013). In contrast, our study using REGγ-KO mice revealed a hepatic steatosis resistance phenotype under HFD conditions. Triple-REG-KO activates an unfolded protein response and increases ER stress in the liver, whereas REGγ-KO does not affect ER homeostatsis. Overexpression of REGγ but not REGα/β led to lipid accumulation. Furthermore, REGγ-KO led to a markedly increased LC3-II accumulation and reduced p62, whereas the effect of REGγ deficiency is not compensated by REGα/β overexpression. Since REGα/β and REGγ have been reported to play distinct biological roles, with many functions still unknown, it is likely that simultaneous knockout of three genes may be too complicated and too early for us to understand the full mechanisms.

Our study demonstrates that REGγ promotes SirT1 degradation in an Ub-independent manner. A previous report suggested that JNK1 phosphorylates SirT1 and promotes its Ub-dependent degradation (Gao et al., 2011). Therefore, SirT1 can be degraded via both Ub-dependent and -independent pathways. In addition, we also revealed that GD induces SirT1 phosphorylation on T530. We estimated the status of SirT1-T530 phosphorylation under physical conditions in mouse hepatocytes and revealed that ~25% of total SirT1 can be phosphorylated on T530 (T522 in mouse) (data not shown). These observations provide a possible explanation for why overexpression of a phospho-deficient SirT1-T530A mutant exhibited no significant effect to its association with REGγ, whereas phosphorylation-mimetic SirT1-T530D mutant markedly reduced its association with REGγ (Figures 7G and 7I). Furthermore, we found that HFD treatment led to a reduction in hepatic levels of SirT1-T530 phosphorylation coupled with a reduction in total SirT1 expression (Figure S7E). Further study on posttranslational modification of SirT1 under different conditions may provide new insights into the SirT1 regulatory network.

Acetylation is emerging as an important autophagy regulatory mechanism. Tip60 (yeast Esa1) acetylase-mediated Atg1 and Atg3 acetylation can induce autophagy (Lin et al., 2012; Yi et al., 2012), P300 acetylase-mediated acetylation of Atg5/Atg7 led to autophagy inhibition (Lee and Finkel, 2009), and SirT1 deacetylase induces autophagy via deacetylation of Atg5/Atg7/Atg8 proteins (Lee et al., 2008). Upon nitrogen starvation, autophagy can be induced by Esa1 via Atg3 acetylation (Yi et al., 2012). Serum starvation triggers signaling from GSK3 to TIP60 to stimulate Atg1 acetylation and autophagy (Lin et al., 2012). In our study, glucose starvation induces AMPK-dependent SirT1 phosphorylation on T530, which entails SirT1-REGγ dissociation and thus releases SirT1 to stimulate autophagy. Interestingly, we detected no significant reduction of REGγ-SirT1 binding after serum starvation (data not shown). These observations proved that cells use distinct acetylation/deacetylation signaling pathways to regulate autophagy in response to different metabolism changes. Collectively, our observations indicate that REGγ forms a complex with SirT1 and serves as an important molecular switch for the off/on regulation of autophagy under normal and energy-deprivation conditions.

In conclusion, the present study establishes a molecular crosstalk between the proteasome activator REGγ and SirT1 signaling in the regulation of autophagy and hepatocyte lipid metabolism. Furthermore, unpublished data in our laboratory also revealed that REGγ-deficient mice exhibit enhanced insulin sensitivity. Thus, it is tempting to speculate that downregulation

of REGγ also may protect against diabetes. Our findings that REGγ regulates autophagy and lipid metabolism make it an attractive drug target since pharmacological manipulation of REGγ could have potential benefits for metabolic disorders such as liver steatosis, diabetes, and age-related diseases.

EXPERIMENTAL PROCEDURES

Animal Experimentation

REGγ KO mice were kindly provided by Dr. John J. Monaco at University of Cincinnati (Barton et al., 2004). All mice used were C57BL/6 male mice. REGγ-WT and -KO mice were fed either with a standard CD or with a HFD (D12492 with 60 kcal% fat; Research Diets, Inc.) starting when the mice were 3 weeks of age and for a total of 19 additional weeks. Animals are treated according to high ethical and scientific standards with oversight by the Animal Center at East China Normal University.

Measurement of Liver/Body Weight and Food Intake

Mice had ad libitum access to either normal CD or HFD and water. Food intake of REGγ-WT or REGγ-KO male mice (n = 4) on HFD was monitored weekly at 17–18 weeks (one pair of REGγ-WT and -KO littermate mice monitored 1 week, the other three pairs monitored for 2 weeks) after HFD. Body weight was determined every 2 weeks. Mouse liver/body weight was measured after being sacrificed.

Cell Lines, Plasmids, and Reagents

HeLa, H1299, HepG2, HEK293T, REGγ-WT, and REGγ-KO MEF cells were maintained in DMEM with 10% fetal bovine serum. REGγ-knockdown, SirT1-knockdown, or vector control stable cell lines were established by transient transfection and selected with puromycin. Primary hepatocytes were isolated as described previously (Liu et al., 2012). GFP-LC3 and Myc-Atg5/Atg7/Atg8 plasmids were kind gifts from Toren Finkel (NIH). SirT1-knockdown plasmids were previously generated (Wang et al., 2006). Cycloheximide, 2DG, AMPK activator (AICAR), and inhibitor (Compound C) were obtained from Sigma. Antibodies were purchased from Sigma (LC3, p62, REGγ, Flag-tag, and β-actin), Santa Cruz Biotechnology (GFP, SirT1, and Myc-tag), Cell Signaling Technology (Ac-K-103-lysine), and Vector Laboratories (goat anti-rabbit IgG).

Analysis of Autophagy by Microscopy

Autophagy was visualized by GFP-LC3 transfection followed by confocal microscopy. For electron microscopy investigations, cells or liver tissues were fixed with 2.5% glutaraldehyde for 3 hr, rinsed in PBS, postfixed in 1% OsO4, dehydrated, and embedded in Epon. Ultrathin sections were contrasted with uranyl acetate and lead citrate and photographed in a JEM-2100 transmission electron microscope.

Immunostaining

Immunohistochemical staining in tissues was performed using anti-SirT1 antibody and visualized as previously described (Liu et al., 2010).

Immunoprecipitation and GST Pull-Down Assay

Cell lysate preparation, protein immunoprecipitation, and GST pull-down assay were performed as previously described (Hu et al., 2012).

Lipid Accumulation and Measurement

Cells were incubated in the absence or presence of sodium oleate or oleate/palmitate (2:1) in culture medium supplemented with 1% fatty acid-free BSA. To measure TG, the lipids were extracted from cell lysates using a chloroform/methanol (2:1) mixture. TG was determined using Serum Triglyceride Determination Kit (TR0100, Sigma). For lipid droplet staining, cells were fixed with 10% formalin and stained with oil red O working solution and visualized under the bright-field microscope. Alternatively, BODIPY 493/503 (0.01 mg/ml) in PBS was applied to lipid droplet stain for 15 min and visualized by fluorescence microscopy. Hepatic TGs were extracted as previously described (Liu et al., 2012). Blood samples were obtained for serum TG measurements.

Statistical Analyses

Results are shown as mean ± SD. Differences were considered significant with a p value < 0.05 using Student's two-tailed t test.

SUPPLEMENTAL INFORMATION

Supplemental Information includes seven figures and Supplemental Experimental Procedures and can be found with this article online at http://dx.doi.org/10.1016/j.cmet.2013.08.012.

ACKNOWLEDGMENTS

This work was supported in part by National Institutes of Health (R01CA131914 to X.L., R01HL51586 to L.C., and NICHD-HD8188 to B.W.O), Norman Hackerman Advanced Research Program (1082318401) and the Pilot/Feasibility Program of the Diabetes Research Center at Baylor College of Medicine (P30-DK079638) to X.L., Cancer Prevention & Research Institute of Texas Core Facility Support Awards (RP120092) and NCI Cancer Center Support Grant to the Proteomics Shared Resource (P30CA125123) to D.P.E., and grants from National Natural Science Foundation of China (31201044, 31071248, 31171361, 81372146, 81261120555, and 81071657), National Basic Research Program of China (2009CB918401, 2009CB918402, and 2011CB504200), and the Science and Technology Commission of Shanghai Municipality (11DZ2260300). The authors would like to thank Mrs. Myra Costello at the Proteomics Shared Resource for her technical support.

Received: February 21, 2013
Revised: June 22, 2013
Accepted: August 9, 2013
Published: September 3, 2013

REFERENCES

Barton, L.F., Runnels, H.A., Schell, T.D., Cho, Y., Gibbons, R., Tevethia, S.S., Deepe, G.S., Jr., and Monaco, J.J. (2004). Immune defects in 28-kDa proteasome activator gamma-deficient mice. J. Immunol. *172*, 3948–3954.

Bernier, M., Paul, R.K., Martin-Montalvo, A., Scheibye-Knudsen, M., Song, S., He, H.J., Armour, S.M., Hubbard, B.P., Bohr, V.A., Wang, L., et al. (2011). Negative regulation of STAT3 protein-mediated cellular respiration by SIRT1 protein. J. Biol. Chem. *286*, 19270–19279.

Brunet, A., Sweeney, L.B., Sturgill, J.F., Chua, K.F., Greer, P.L., Lin, Y., Tran, H., Ross, S.E., Mostoslavsky, R., Cohen, H.Y., et al. (2004). Stress-dependent regulation of FOXO transcription factors by the SIRT1 deacetylase. Science *303*, 2011–2015.

Chen, W.Y., Wang, D.H., Yen, R.C., Luo, J., Gu, W., and Baylin, S.B. (2005). Tumor suppressor HIC1 directly regulates SIRT1 to modulate p53-dependent DNA-damage responses. Cell *123*, 437–448.

Czaja, M.J. (2010). Autophagy in health and disease. 2. Regulation of lipid metabolism and storage by autophagy: pathophysiological implications. Am. J. Physiol. Cell Physiol. *298*, C973–C978.

Ding, W.X., Ni, H.M., Gao, W., Hou, Y.F., Melan, M.A., Chen, X., Stolz, D.B., Shao, Z.M., and Yin, X.M. (2007a). Differential effects of endoplasmic reticulum stress-induced autophagy on cell survival. J. Biol. Chem. *282*, 4702–4710.

Ding, W.X., Ni, H.M., Gao, W., Yoshimori, T., Stolz, D.B., Ron, D., and Yin, X.M. (2007b). Linking of autophagy to ubiquitin-proteasome system is important for the regulation of endoplasmic reticulum stress and cell viability. Am. J. Pathol. *171*, 513–524.

Dubiel, W., Pratt, G., Ferrell, K., and Rechsteiner, M. (1992). Purification of an 11 S regulator of the multicatalytic protease. J. Biol. Chem. *267*, 22369–22377.

Fu, S., Yang, L., Li, P., Hofmann, O., Dicker, L., Hide, W., Lin, X., Watkins, S.M., Ivanov, A.R., and Hotamisligil, G.S. (2011). Aberrant lipid metabolism disrupts calcium homeostasis causing liver endoplasmic reticulum stress in obesity. Nature *473*, 528–531.

Fu, S., Fan, J., Blanco, J., Gimenez-Cassina, A., Danial, N.N., Watkins, S.M., and Hotamisligil, G.S. (2012). Polysome profiling in liver identifies dynamic

regulation of endoplasmic reticulum translatome by obesity and fasting. PLoS Genet. *8*, e1002902.

Gao, Z., Zhang, J., Kheterpal, I., Kennedy, N., Davis, R.J., and Ye, J. (2011). Sirtuin 1 (SIRT1) protein degradation in response to persistent c-Jun N-terminal kinase 1 (JNK1) activation contributes to hepatic steatosis in obesity. J. Biol. Chem. *286*, 22227–22234.

Guarente, L. (2000). Sir2 links chromatin silencing, metabolism, and aging. Genes Dev. *14*, 1021–1026.

Hu, C., Zhang, S., Gao, X., Gao, X., Xu, X., Lv, Y., Zhang, Y., Zhu, Z., Zhang, C., Li, Q., et al. (2012). Roles of Kruppel-associated Box (KRAB)-associated Co-repressor KAP1 Ser-473 Phosphorylation in DNA Damage Response. J. Biol. Chem. *287*, 18937–18952.

Korolchuk, V.I., Mansilla, A., Menzies, F.M., and Rubinsztein, D.C. (2009). Autophagy inhibition compromises degradation of ubiquitin-proteasome pathway substrates. Mol. Cell *33*, 517–527.

Kroemer, G., Mariño, G., and Levine, B. (2010). Autophagy and the integrated stress response. Mol. Cell *40*, 280–293.

Lee, I.H., and Finkel, T. (2009). Regulation of autophagy by the p300 acetyltransferase. J. Biol. Chem. *284*, 6322–6328.

Lee, I.H., Cao, L., Mostoslavsky, R., Lombard, D.B., Liu, J., Bruns, N.E., Tsokos, M., Alt, F.W., and Finkel, T. (2008). A role for the NAD-dependent deacetylase Sirt1 in the regulation of autophagy. Proc. Natl. Acad. Sci. USA *105*, 3374–3379.

Li, X., Lonard, D.M., Jung, S.Y., Malovannaya, A., Feng, Q., Qin, J., Tsai, S.Y., Tsai, M.J., and O'Malley, B.W. (2006). The SRC-3/AIB1 coactivator is degraded in a ubiquitin- and ATP-independent manner by the REGgamma proteasome. Cell *124*, 381–392.

Li, X., Amazit, L., Long, W., Lonard, D.M., Monaco, J.J., and O'Malley, B.W. (2007). Ubiquitin- and ATP-independent proteolytic turnover of p21 by the REGgamma-proteasome pathway. Mol. Cell *26*, 831–842.

Lin, S.Y., Li, T.Y., Liu, Q., Zhang, C., Li, X., Chen, Y., Zhang, S.M., Lian, G., Ruan, K., Wang, Z., et al. (2012). GSK3-TIP60-ULK1 signaling pathway links growth factor deprivation to autophagy. Science *336*, 477–481.

Liu, J., Yu, G., Zhao, Y., Zhao, D., Wang, Y., Wang, L., Liu, J., Li, L., Zeng, Y., Dang, Y., et al. (2010). REGgamma modulates p53 activity by regulating its cellular localization. J. Cell. Sci. *123*, 4076–4084.

Liu, Y., Zhou, D., Zhang, F., Tu, Y., Xia, Y., Wang, H., Zhou, B., Zhang, Y., Wu, J., Gao, X., et al. (2012). Liver Patt1 deficiency protects male mice from age-associated but not high-fat diet-induced hepatic steatosis. J. Lipid Res. *53*, 358–367.

Liu, J., Wang, Y., Li, L., Zhou, L., Wei, H., Zhou, Q., Liu, J., Wang, W., Ji, L., Shan, P., et al. (2013). Site-specific acetylation of the proteasome activator REGγ directs its heptameric structure and functions. J. Biol. Chem. *288*, 16567–16578.

Luo, J., Nikolaev, A.Y., Imai, S., Chen, D., Su, F., Shiloh, A., Guarente, L., and Gu, W. (2001). Negative control of p53 by Sir2alpha promotes cell survival under stress. Cell *107*, 137–148.

Ma, C.P., Slaughter, C.A., and DeMartino, G.N. (1992). Identification, purification, and characterization of a protein activator (PA28) of the 20 S proteasome (macropain). J. Biol. Chem. *267*, 10515–10523.

Mizushima, N. (2007). Autophagy: process and function. Genes Dev. *21*, 2861–2873.

Murata, S., Kawahara, H., Tohma, S., Yamamoto, K., Kasahara, M., Nabeshima, Y., Tanaka, K., and Chiba, T. (1999). Growth retardation in mice lacking the proteasome activator PA28gamma. J. Biol. Chem. *274*, 38211–38215.

Nasrin, N., Kaushik, V.K., Fortier, E., Wall, D., Pearson, K.J., de Cabo, R., and Bordone, L. (2009). JNK1 phosphorylates SIRT1 and promotes its enzymatic activity. PLoS ONE *4*, e8414.

Nemoto, S., Fergusson, M.M., and Finkel, T. (2004). Nutrient availability regulates SIRT1 through a forkhead-dependent pathway. Science *306*, 2105–2108.

Otoda, T., Takamura, T., Misu, H., Ota, T., Murata, S., Hayashi, H., Takayama, H., Kikuchi, A., Kanamori, T., Shima, K.R., et al. (2013). Proteasome dysfunction mediates obesity-induced endoplasmic reticulum stress and insulin resistance in the liver. Diabetes *62*, 811–824.

Pfluger, P.T., Herranz, D., Velasco-Miguel, S., Serrano, M., and Tschöp, M.H. (2008). Sirt1 protects against high-fat diet-induced metabolic damage. Proc. Natl. Acad. Sci. USA *105*, 9793–9798.

Picard, F., Kurtev, M., Chung, N., Topark-Ngarm, A., Senawong, T., de Oliveira, R.M., Leid, M., McBurney, M.W., and Guarente, L. (2004). Sirt1 promotes fat mobilization in white adipocytes by repressing PPAR-gamma. Nature *430*, 921–921.

Purushotham, A., Schug, T.T., Xu, Q., Surapureddi, S., Guo, X.M., and Li, X.L. (2009). Hepatocyte-specific deletion of SIRT1 alters fatty acid metabolism and results in hepatic steatosis and inflammation. Cell Metab. *9*, 327–338.

Qiang, L., Wang, L.H., Kon, N., Zhao, W.H., Lee, S., Zhang, Y.Y., Rosenbaum, M., Zhao, Y.M., Gu, W., Farmer, S.R., and Accili, D. (2012). Brown remodeling of white adipose tissue by SirT1-dependent deacetylation of Pparγ. Cell *150*, 620–632.

Salem, M., Silverstein, J., Rexroad, C.E., 3rd, and Yao, J. (2007). Effect of starvation on global gene expression and proteolysis in rainbow trout (Oncorhynchus mykiss). BMC Genomics *8*, 328.

Singh, R., and Cuervo, A.M. (2012). Lipophagy: connecting autophagy and lipid metabolism. Int. J. Cell Biol. *2012*, 282041.

Singh, R., Kaushik, S., Wang, Y., Xiang, Y., Novak, I., Komatsu, M., Tanaka, K., Cuervo, A.M., and Czaja, M.J. (2009). Autophagy regulates lipid metabolism. Nature *458*, 1131–1135.

Sinha, R.A., You, S.H., Zhou, J., Siddique, M.M., Bay, B.H., Zhu, X., Privalsky, M.L., Cheng, S.Y., Stevens, R.D., Summers, S.A., et al. (2012). Thyroid hormone stimulates hepatic lipid catabolism via activation of autophagy. J. Clin. Invest. *122*, 2428–2438.

Wang, C., Chen, L., Hou, X., Li, Z., Kabra, N., Ma, Y., Nemoto, S., Finkel, T., Gu, W., Cress, W.D., and Chen, J. (2006). Interactions between E2F1 and SirT1 regulate apoptotic response to DNA damage. Nat. Cell Biol. *8*, 1025–1031.

Wójcik, C. (1999). Proteasome activator subunit PA28 alpha and related Ki antigen (PA28 gamma) are absent from the nuclear fraction purified by sucrose gradient centrifugation. Int. J. Biochem. Cell Biol. *31*, 273–276.

Yang, L., Li, P., Fu, S.N., Calay, E.S., and Hotamisligil, G.S. (2010). Defective hepatic autophagy in obesity promotes ER stress and causes insulin resistance. Cell Metab. *11*, 467–478.

Yi, C., Ma, M., Ran, L., Zheng, J., Tong, J., Zhu, J., Ma, C., Sun, Y., Zhang, S., Feng, W., et al. (2012). Function and molecular mechanism of acetylation in autophagy regulation. Science *336*, 474–477.

Zhang, Y., Goldman, S., Baerga, R., Zhao, Y., Komatsu, M., and Jin, S.K. (2009). Adipose-specific deletion of autophagy-related gene 7 (atg7) in mice reveals a role in adipogenesis. Proc. Natl. Acad. Sci. USA *106*, 19860–19865.

Zhao, W., Kruse, J.P., Tang, Y., Jung, S.Y., Qin, J., and Gu, W. (2008). Negative regulation of the deacetylase SIRT1 by DBC1. Nature *451*, 587–590.